J. Condensed Matter Nucl. Sci. 37 (2023) 68–83

Research Article

Hydrogen Embrittlement, Microcracking, and THz Vibrations in the Metal Electrodes of Cold-Fusion Electrolysis Experiments: Repeatability of Nuclear and Stoichiometric Balances

Alberto Carpinteri*, Oscar Borla, Amedeo Manuello

Politecnico di Torino, Department of Structural, Geotechnical and Building Engineering, Corso Duca degli Abruzzi 24 – 10129 Torino, Italy

Abstract

In the last few decades, several scientific papers have reported experimental evidence of anomalous nuclear reactions occurring in condensed matter during electrolytic phenomena or mechanical instabilities such as fracture (in solids) and cavitation (in liquids). Despite the numerous research activities carried out in the field of so-called "Cold Nuclear Fusion", this phenomenon remains today not fully understood. In recent contributions by the authors, the formation of cracks on the surface of the electrodes used during electrolysis tests, together with chemical composition variations and anomalous sub-atomic particle emissions, were described. A mechanical interpretation of the experimental evidence can be based on low-energy phono-fission reactions, which are a consequence of hydrogen embrittlement, microcracking, and THz vibrations. In the present paper, the repeatable results of different laboratory testing programs obtained by means of Pd and Ni are discussed. Preliminary short notes about the energy balance close the paper.
 ISSN 2227-3123

Keywords: Hydrogen embrittlement; microcracking; THz vibrations; cold fusion; electrolysis; phono-fission reactions; neutron and alpha particle emission; energy balance; nuclear and stoichiometric balances

1. Introduction

Since the 1920s, it has been hypothesized that nuclear fusion could occur by hydrogen absorption in a metal catalyst [1] *at temperatures much lower than tens of million degrees required for plasma fusion*.

In the present paper, the authors propose a totally different interpretation of the phenomenon usually called "Cold Nuclear Fusion". The Helium atoms produced during cold fusion will be shown to be fragments from fission reactions (alpha particles) and not products from Hydrogen or Deuterium nuclear fusion.

Among the several experiments conducted in this research field, the most relevant statements about cold fusion were made by Stanley Pons and Martin Fleischmann in 1989 [2]. Their conjecture was that the high compression ratio

*Corresponding author: alberto.carpinteri@polito.it

 ISSN 2227-3123

and the mobility of Deuterium (a stable isotope of hydrogen) during electrolysis might result in an unexpected nuclear fusion. In particular, their experiments were carried out by means of a palladium cathode and heavy water (D_2O) placed inside a thermally insulated calorimeter in order to measure the heat produced by the electrolytic process. The electrical power supply was continuously applied and the heavy water was renewed at regular intervals [2]. For most of the time, the power absorbed by the cell was equal to the calculated output power, within the measurement accuracy and the cell temperature was stable around 30°C. However, in some experiments, the temperature suddenly increased to about 50°C without changes in the input power [2]. In support of the presumed occurrence of nuclear reactions giving rise to the temperature increase, Fleischmann and Pons reported the presence of neutrons and tritium [2].

In 1998, Mizuno and Ohmori [3], [4] announced the possibility of obtaining cold fusion reactions without using palladium or heavy water, but only through tungsten electrodes immersed in a solution of common water and potassium carbonate (K_2CO_3). By applying voltage ranging from 160 up to 300 V, the temperature of the solution exceeded [70-80]°C and a plasma bubble formed around the immersed portion of the tungsten electrode. Then, a positive energy balance was estimated with a thermal energy emission 20–100% above the electrical energy used to trigger the reaction. Moreover, several medium-weight elements like calcium, titanium, chromium, manganese, iron, cobalt, copper, and zinc were observed on the cathode, which were not present before operating the electrolytic cell [5].

In 2007, Mosier-Boss et al. [6], [7] obtained important evidence of anomalous heat generation, alpha particle emissions, and compositional changes during electrolysis experiments by means of a palladium cathode immersed in a solution of lithium chloride and deuterated water. As in the case of Mizuno et al. [5], elements such as Fe, Cr, Ni, and Al were detected at the end of the tests [8]. To explain the formation of these new elements, Mosier-Boss and co-authors suggested a multi-body deuteron fusion phenomenon and the palladium lattice disintegration [8].

In addition to the experimental results described above, many other examples of unexpected nuclear reactions in condensed matter have been reported by various authors [9]–[36]. All of these tests are characterized by anomalous heat generation, and many by neutron and alpha particle emissions as well. Furthermore, some of the authors cited significant examples of compositional variations and micro-cracking of the electrodes [3], [4], [30]–[32].

Many years ago, Preparata commented: “despite the great amount of experimental results observed by a large number of scientists, a unified interpretation and theory of these phenomena has not been accepted and their comprehension still remains unsolved” [19], [20].

However, as discussed in many subsequent cold fusion papers, one of the features common to many experiments is the appearance of microcracks on electrode surfaces after the tests: i.e. the common environment in which low-energy nuclear reactions occur is proposed to be cracks of a critical size followed by a resonance process that dissipates energy from those sites [30], [31]. Such evidence might be directly correlated to hydrogen embrittlement of the material composing the metal electrodes. This phenomenon, well-known in Metallurgy and Fracture Mechanics, characterizes metals during forming or finishing operations [37].

Recent innovative experiments provided strong evidence of anomalous fission reactions and nuclear transmutations occurring in condensed matter, not only during electrolysis tests, but also during fracture of solids and in cavitation of liquids [38]–[46]. Based on these experimental observations, a mechanical explanation for the so-called cold nuclear fusion is suggested [38], [46].

Hydrogen embrittlement seems to play an essential role in the observed microcracking of the electrode host metals (Pd, Ni, Fe, etc.). In particular, the metal matrix is subjected to mechanical damaging and fracturing due to hydrogen atoms (produced by the electrolysis itself) penetrating into the atomic lattice and expanding it during gas loading. The hydrogen atoms generate an internal compression stress that apparently lowers the fracture toughness of the metal, so that brittle crack growth can occur with a hydrogen partial pressure below 1 atm [38]. Consequently, the hypothesis is that phono-fission reactions may occur in correspondence to nano- and microcrack formation or propagation [38]. THz phonons are, in fact, produced at the nano-scale showing a frequency equivalent to that of thermal neutrons, and are able to trigger fission reactions on medium-weight elements. As a matter of fact, thermal neutrons are characterized by

a frequency of 6.05 THz (according to the well-known law that links energy and frequency through Planck's constant), which is very close to the uranium atomic lattice resonance frequency (Debye frequency) of 6.24 THz, as well as to that of Fe (7.77 THz) and Ca (4.79 THz).

These new kinds of reactions have also been observed from the laboratory to the Earth's crust when particular pressure waves originate from fracture phenomena as well as before or in correspondence to seismic events [38], [40]–[45], [47]–[54]. Theoretical explanations for this anomalous nuclear phenomenon are described in some papers recently published [38], [55]–[59].

In the present study, the results of phono-fission reactions during electrolysis tests are presented. In order to confirm the earlier results obtained by Co-Cr and Ni-Fe electrodes [38], [46], as well as by Pd and Ni electrodes (Test 1) [38], [46], three new electrolytic experiments (Test 2, Test 3, and Test 4) have been conducted using 100% palladium cathodes. These new experimental tests intend to emphasize the repeatability of the physical phenomenon and to deeply understand the different phases that characterize the experiments and the various catalyzing factors. For these reasons, the three further series of tests were arranged in three trials each, with a duration of 2.5, 5, and 10 hours. This protocol was adopted to evaluate whether the chemical variations observed in the previous experiments are concentrated during a single trial or whether they are distributed throughout the entire duration of the test.

The experimental results, published in this paper for the first time, show significant neutron emissions together with relevant compositional changes and the appearance of previously absent chemical elements. Moreover, evident micro- and macrocracks of the electrodes were observed, thus emphasizing not only the strong repeatability, but also the mechanical origin of the phenomenon.

Further experimental evidence of fracture and shredding of copper and tungsten cathode wires during electrolysis experiments has recently been described by Widom et al. [60], [61].

A preliminary energy balance evaluation has also been performed using a thermographic camera for temperature variation monitoring, a specially designed electrical power meter, and by estimation of the evaporated aqueous solution produced during electrolysis. In particular, the latent heat of evaporation, the convective heat transfer, and the Stefan-Boltzmann thermal radiation have been considered in the energy balance evaluation.

2. Experimental Set-Up

Over the last ten years,experiments have been conducted using an electrolytic reactor (owners: Mr. A. Goi et al.) to investigate whether the anomalous heat generation may be correlated to a new type of nuclear reaction occurring during electrolysis [38], [46].

The experimental device when filled with a salt solution of water and potassium carbonate (K_2CO_3), triggers the electrolytic phenomenon by using two metal electrodes immersed in the aqueous solution (Fig. 1).

The solution container, or reaction chamber is an AISI 316L steel cylinder, 100 mm in diameter, 150 mm in height, with a wall thickness of 5 mm.

The base of the chamber consists of a ceramic plate preventing the direct contact between the liquid solution and Teflon lid. Two threaded holes secure the electrodes, which are screwed into the bottom of the chamber. A valve at the top of the cell allows the gas to escape from the reactor and to condense in an external collector. Externally, two circular Inox steel flanges, fastened by means of four threaded supports, hold the Teflon layers. The interior steel flange of the reactor is connected to four supports isolated from the ground by means of a rubber-based material.

The voltage supply is provided by means of a RTS40CE dimmer connected to the 220 VDC mains power line and sets the voltage using a potentiometer. In order to obtain a pulsating direct voltage/current (VDC), a diode bridge rectifier was added to the output of the RTS40CE. All the electrical parameters were monitored during the tests by a virtual multimeter specially programmed for the experimentation.

Figure 1. Experimental set-up (a); Pd and Ni Electrodes (b).

During the experiments discussed in this paper, the Pd electrode was employed as cathode (negative pole), whereas the Ni electrode for the anode (positive pole).

The electrolytic cell was switched from low to high by letting the current and voltage vary in the range of 3 to 5 A and 20 to 120 V, respectively.

Neutron emission was monitored using a He^3 proportional counter with pre-amplification, amplification, and discrimination electronics directly connected to the detector tube (see Fig. 1a). The detector was supplied with a high voltage of $\sim$ 1.3 kV via a Nuclear Instrument Module (NIM). The logic output producing the TTL (transistor–transistor logic) pulses was connected to a NIM counter. The logic output of the detector was enabled for analog signals exceeding 300 mV. This discrimination threshold is a consequence of the sensitivity of the He^3 detector to the gamma rays produced during neutron emission in ordinary nuclear processes. This value was determined by measuring the analog signal of the detector using a Co-60 gamma source. The detector was also calibrated at the factory for the measurement of thermal neutrons; its sensitivity is 65 cps/n_{thermal} ($\pm 10\%$ according to the manufacturer); so, the flux of thermal neutrons is one thermal neutron/s cm^2, corresponding to a count rate of 65 cps.

Finally, before and after the experiments, Energy Dispersive X-ray Spectroscopy was carried out in order to identify possible direct evidence of phono-fission reactions that can take place during the electrolysis. The elemental analyses were performed by a ZEISS Auriga field emission scanning electron microscope (FESEM) equipped with an Oxford INCA energy-dispersive X-ray detector (EDX), with a resolution of 124 eV @ MnKa. The energy used for the analyses was 18 keV.

3. Neutron Emission Measurements

Neutron emission monitoring performed during the first experimental activity on Pd and Ni electrodes (Test 1) [38] is shown in Fig. 2. The measurement performed by the He3 detector was conducted for a total time of about 20 hours. The background level was equal to $(3.23 \pm 1.49) \times 10^{-2}$ cps.

After about 7.5 hours (460 minutes), a neutron flux of about 3 times the background level was detected [38]. Similarly, after 9 hours (545 minutes) from the beginning of the test, an emission level of about one order of magnitude greater than the background was observed. Finally, after 20 hours (1200 minutes), another neutron peak up to 7 times

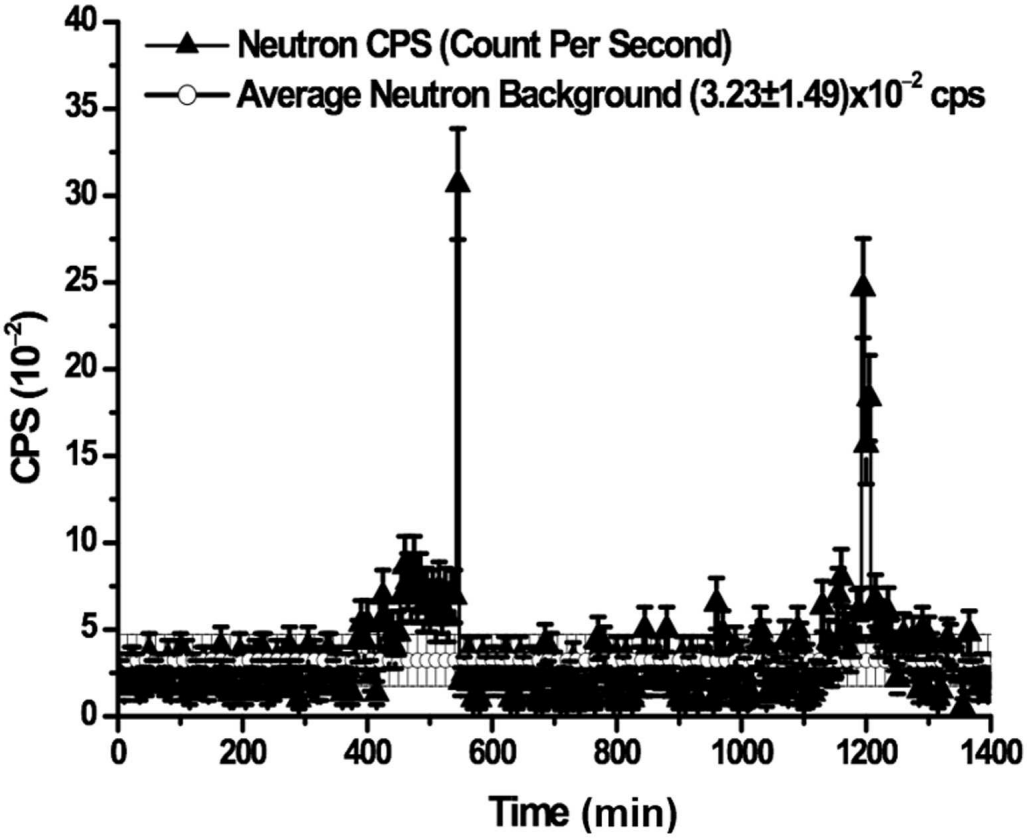

Figure 2. Neutron emission measurements detected during the first experimental test (Test 1) with a time duration of 20 hours using Pd and Ni electrodes.

the background was measured. More details about this experimental test can be found in a previous publication by the lead author [38].

The neutron emissions monitored during the second experimental test (Test 2) are reported in Fig. 3 as an example. In particular, the neutron levels obtained during the three time intervals of 2.5, 5, and 10 hours are shown.

A neutron background of (6.00±2.45) $\times 10^{-2}$ cps was measured for the first two intervals (2.5 and 5 hours), while neutron peaks about 2 times (Fig. 3a) and 5 times (Fig. 3c) higher were observed just before switching off the cell.

As additional supporting evidence, the cumulative count curves were compared to the cumulative average background level (see Fig. 3b, d). Using this method, it is possible to observe how in the former case the neutron emission is comparable with the background level. Conversely, in the latter case, the cumulative curve appears to be significantly higher, suggesting that the anomalous neutron emission takes place after an incubation time, and not immediately after the cell switches on. This behavior is more evident when analyzing in detail the results obtained during the third experimental interval lasting 10 hours. In this case, the environmental background was found to be equal to (7.85±1.62) $\times 10^{-2}$ cps. After about 80 minutes from the beginning of the test, neutron emissions greater than the background

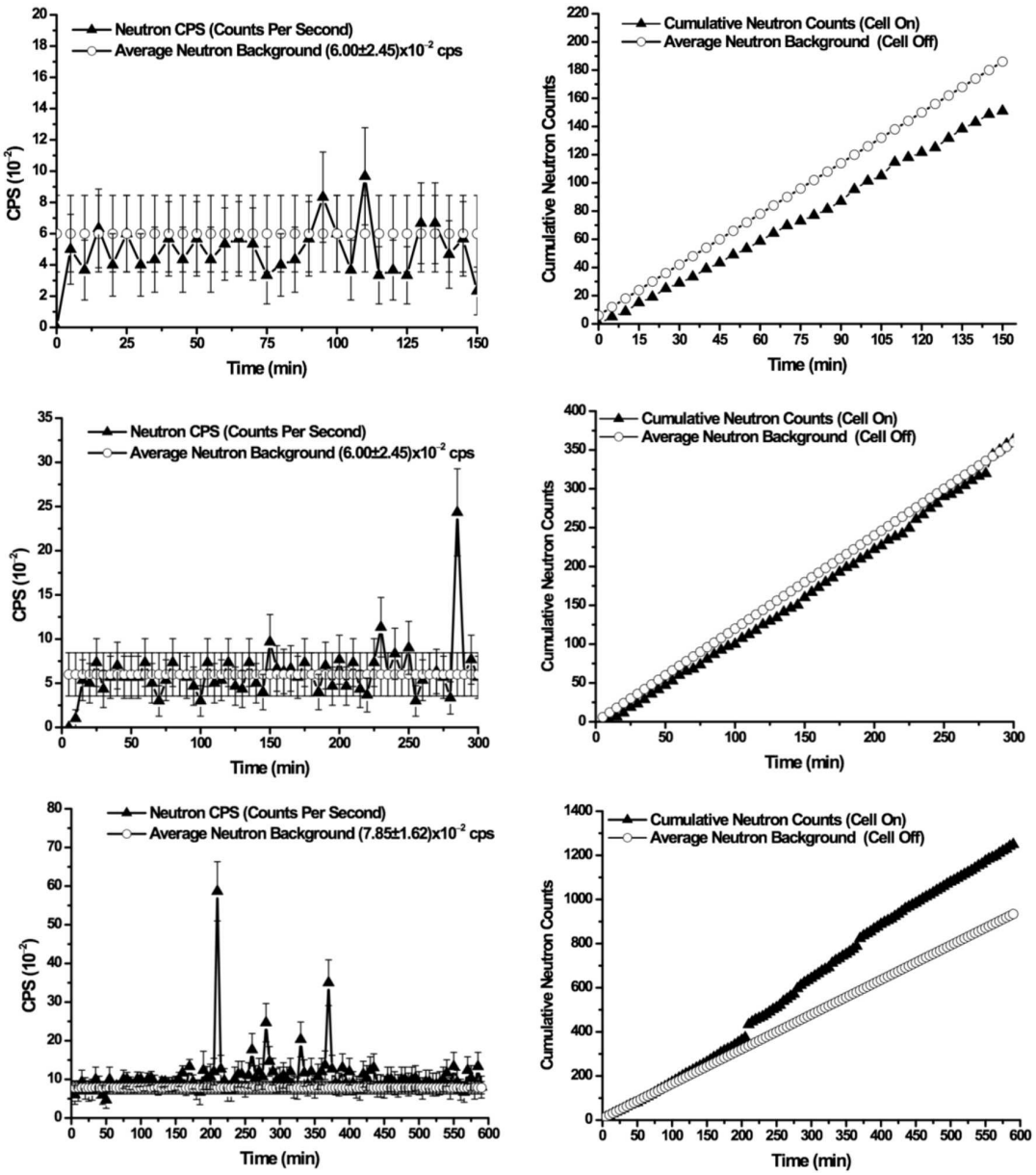

Figure 3. Neutron emission measurements for the second test on Pd and Ni electrodes (Test 2) after 2.5 hours (a); 5 hours (c); and 10 hours (e); cumulated curve of CPS compared to the cumulated average background level are reported for the same durations (b), (d), (f).

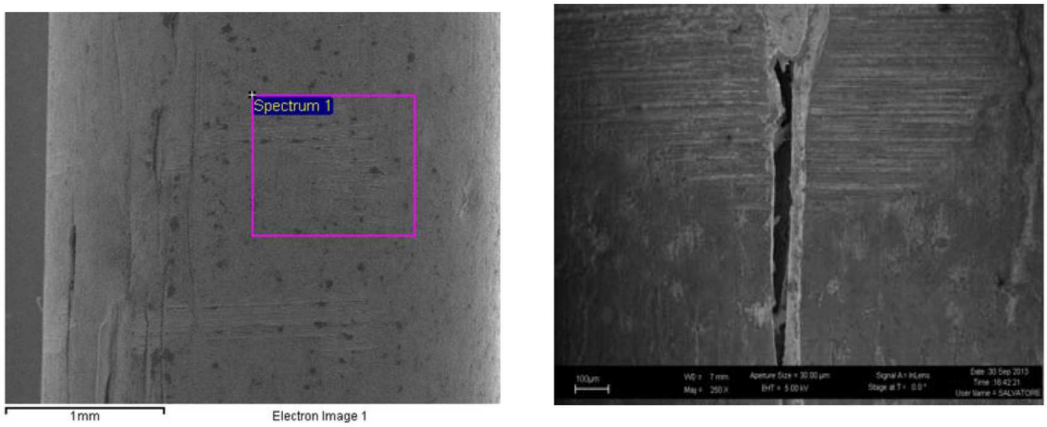

Figure 4. Image of the Pd electrode before the experiment (a). The electrode after many operating hours presented cracks of about 40 μm width observable at naked eyes (b).

level were detected (Fig. 3e). In particular, after 200 minutes and up to 400 minutes, neutron peaks greater than ten times the background were measured. This evidence can also be observed in the cumulative curve shown in figure 3f.

The observed behavior appears to be consistent with claims made by Fleishmann and Pons and other researchers: anomalous emissions and energy were concentrated in some periods of an experiment, but not continuously distributed over its duration [2]–[5].

4. Chemical Composition Analysis

In this section, the chemical composition analyses performed before and after all the experiments on Pd and Ni electrodes are summarized. The reported percentages represent the average values based on 15 independent measurements performed in different equidistant locations along each metallic electrode, 40 mm in length.

The hydrogen embrittlement hypothesis, based on the presence of micro and mesocracks on the electrode surface, supports the mechanical interpretation of the phenomenon [38], [46]. On the Pd electrode, where a mesoscopic fracture took place during the test, the crack presented an opening displacement of about 40 μm and a length of a few millimeters (see Figures 4a and 4b).

Palladium is widely utilized in the experiments related to so-called cold fusion due to its hydrogen absorption and embrittlement capability. The authors experimented for the first time with Pd and Ni electrodes in a test of 20 hours (Test 1) [38], [46]. The most impressive result in this case was the huge Pd depletion, with a final decrease of 28.7%, and the appearance of chemical elements absent before the test (Fe, Ca, O, Si, K) [38], [46]. Additionally, a total decrease in nickel content of 23.1% was measured on the Ni electrode.

In particular, considering the average decline in Pd (-28.7%) after 20 hours, reported in Tables 1a-c, according to [38] and to the phono-fission hypothesis, the following reaction can be postulated:

$$\mathrm{Pd}_{46}^{106} \rightarrow \mathrm{Ca}_{20}^{40} + \mathrm{Fe}_{26}^{56} + 10\ \mathrm{neutrons} \tag{1}$$

Referring to reaction (1), the Pd decline of 28.7% can be counterbalanced by the Ca and Fe increases of 10.8% and 15.2%, respectively (see Tables 1a-c).

Table 1. Test 1 performed on Pd and Ni electrodes. Element concentrations before the experiment, and after 20 hours from the beginning (a), nuclear (b) and stoichiometric (c) balances.

(a)

Pd electrode element concentrations						
	Pd(%)	**O(%)**	**Fe(%)**	**K(%)**	**Si(%)**	**Mg(%)**
Before the experiment	100	0.0	0.0	0.0	0.0	0.0
After 20h	71.3	18.5	2.0	2.0	1.1	1.0

Ni electrode element concentrations					
	Ni(%)	**O(%)**	**Fe(%)**	**Si(%)**	**Al(%)**
Before the experiment	91.6	2.0	2.4	0.3	0.0
After 20h	68.5	21.5	0.4	1.1	1.8

(b)

Pd electrode nuclear balances

$$\mathrm{Pd}_{46}^{106} \rightarrow \mathrm{Ca}_{20}^{40} + \mathrm{Fe}_{26}^{56} + 10\mathrm{n}_{0}^{1}$$
$$\mathrm{Fe}_{26}^{56} \rightarrow 3\mathrm{O}_{8}^{16} + \mathrm{He}_{2}^{4} + 4\mathrm{n}_{0}^{1}$$
$$\mathrm{Ca}_{20}^{40} \rightarrow \mathrm{O}_{8}^{16} + \mathrm{Mg}_{12}^{24}$$
$$\mathrm{Ca}_{20}^{40} \rightarrow 2\mathrm{O}_{8}^{16} + 2\mathrm{He}_{2}^{4}$$
$$\mathrm{Ca}_{20}^{40} \rightarrow \mathrm{K}_{19}^{39} + \mathrm{H}_{1}^{1}$$
$$\mathrm{Ca}_{20}^{40} \rightarrow \mathrm{C}_{6}^{12} + \mathrm{Si}_{14}^{28}$$

Ni electrode nuclear balances

$$\mathrm{Ni}_{28}^{58} \rightarrow 3\mathrm{O}_{8}^{16} + 2\mathrm{He}_{2}^{4} + 2\mathrm{n}_{0}^{1}$$
$$\mathrm{Ni}_{28}^{58} \rightarrow 2\mathrm{Si}_{14}^{28} + 2\mathrm{n}_{0}^{1}$$
$$\mathrm{Fe}_{26}^{56} \rightarrow 2\mathrm{Al}_{13}^{27} + 2\mathrm{n}_{0}^{1}$$
$$\mathrm{Si}_{14}^{20} \rightarrow \mathrm{Al}_{13}^{27} + \mathrm{H}_{1}^{1}$$

(c)

Pd electrode stoichiometric balances

$$\mathrm{Pd}\ (-\ 28.7\%) = \mathrm{Ca}\ (+\ 10.8\%) + \mathrm{Fe}\ (+\ 15.2\%) + \mathrm{n}\ (+\ 2.7\%)$$
$$\mathrm{Fe}\ (-\ 13.2\%) = \mathrm{O}\ (+\ 11.3\%) + \mathrm{He}\ (+\ 0.9\%) + \mathrm{n}\ (+\ 0.9\%)$$
$$\mathrm{Ca}\ (-\ 6.0\%) = \mathrm{O}\ (+\ 4.8\%) + \mathrm{He}\ (+\ 1.2\%)$$
$$\mathrm{Ca}\ (-\ 1.7\%) = \mathrm{O}\ (+\ 0.7\%) + \mathrm{Mg}\ (+\ 1.0\%)$$
$$\mathrm{Ca}\ (-\ 1.5\%) = \mathrm{K}\ (+\ 1.5\%) + \mathrm{H}\ (+\ 0.0\%)$$
$$\mathrm{Ca}\ (-\ 1.6\%) = \mathrm{C}\ (+\ 0.5\%) + \mathrm{Si}\ (+\ 1.1\%)$$

Ni electrode stoichiometric balances

$$\mathrm{Ni}\ (-\ 22.3\%) = \mathrm{O}\ (+\ 18.4\%) + \mathrm{He}\ (+\ 3.1\%) + \mathrm{n}\ (+\ 0.8\%)$$
$$\mathrm{Ni}\ (-\ 0.8\%) = \mathrm{Si}\ (+\ 0.8\%) + \mathrm{n}\ (+\ 0.0\%)$$
$$\mathrm{Fe}\ (-\ 1.8\%) = \mathrm{Al}\ (+\ 1.8\%) + \mathrm{n}\ (+\ 0.0\%)$$

These variations should be accompanied by a neutron emission corresponding to the remaining 2.7% of the mass. The iron increase, according to reaction (1), could be considered as the starting element for the production of other lighter elements. Hence, a second hypothesis can be proposed involving Fe as the starting element and O as the end-product, together with alpha and neutron emissions:

$$\mathrm{Fe}_{26}^{56} \rightarrow 3\mathrm{O}_{8}^{16} + \mathrm{He}_{2}^{4} + 4 \text{ neutrons} \tag{2}$$

According to reaction (2) and considering the residual Fe increment of 2% measured at the end of the test, an iron depletion of 13.2% produces 11.3% of oxygen with alpha particles (He) and neutron emissions. The total measured increase in oxygen after the experiment is equal to 18.5 (see Tables 1a-c). This amount seems to be only partially explained by reaction (2), whereas part of the remaining O concentration could be justified by other reactions involving Ca (generated in reaction 1) as the starting element:

$$\mathrm{Ca}_{20}^{40} \rightarrow \mathrm{O}_{8}^{16} + \mathrm{Mg}_{12}^{24}, \tag{3}$$

$$\mathrm{Ca}_{20}^{40} \rightarrow 2\mathrm{O}_{8}^{16} + 2\mathrm{He}_{2}^{4}. \tag{4}$$

From reaction (3), a decline in Ca concentration of 1.7% with the formation of 1.0% of Mg and 0.7% of O can be considered. From reaction (4), a decline in Ca of 6.0% corresponding to an increase of about 4.8% in O, with alpha particle emissions, is observed. Considering the O increases coming from reactions (2), (3), and (4), combined are equal to 16.8%, and the experimental evidence reporting a total measured O concentration of 18.5%, Oxygen seems to be at least partly implicated in the proposed reaction cascade.

The remaining Ca decline of 3.1% can be explained by the following reactions:

$$\mathrm{Ca}_{20}^{40} \rightarrow \mathrm{K}_{19}^{39} + \mathrm{H}_{1}^{1} \tag{5}$$

$$\mathrm{Ca}_{20}^{40} \rightarrow \mathrm{C}_{6}^{12} + \mathrm{Si}_{14}^{28}. \tag{6}$$

At the same time, the Mg, K and Si increases observed after the experiment can be explained by the reactions (3), (5) and (6).

These nuclear and stoichiometric balances seem to be very interesting, considering they represent a quantitative confirmation of the results previously published [38].

In a similar manner, let us consider the Nickel electrode. Tables 1a-c summarize the concentration variations after electrolysis. The most significant result concerns the nickel depletion equal to 23.1% and the Oxygen increase of about 19.5%.

The following phono-fission reactions (7) and (8), seem to imply neutron and alpha particle emissions, which would also explain the entire Ni decrease and the corresponding O increase:

$$\mathrm{Ni}_{28}^{58} \rightarrow 2\mathrm{Si}_{14}^{28} + 2 \text{ neutrons} \tag{7}$$

$$\mathrm{Ni}_{28}^{58} \rightarrow 3\mathrm{O}_{8}^{16} + \mathrm{He}_{2}^{4} + 2 \text{ neutrons}. \tag{8}$$

On the other hand, Fe (–2.0%) and Al (+1.8%) content variations can be justified by the reaction (9):

$$\mathrm{Fe}_{26}^{56} \rightarrow 2\mathrm{Ai}_{13}^{27} + 2 \text{ neutrons} \tag{9}$$

Considering the experimental results of Tests 2, 3, and 4, published here for the first time, the observed changes in chemical composition were highly repeatable.

The results related to Test 2 are reported in Tables 2 a-c. Please note that only small chemical composition changes were detected in the first two phases (2.5 and 5 hours), whereas a very appreciable Pd depletion (?28.9%) was measured at the end of the 10-hour test. In particular, compositional variations very similar to those observed in the case of the 20-hour experiment (Test 1) were found.

Table 2. Test 2 on Pd and Ni electrodes. Element concentrations before the experiment, and after 2.5, 5, 10 hours from the beginning (a), nuclear (b) and stoichiometric (c) balances.

(a)

Pd electrode element concentrations							
	Pd(%)	**O(%)**	**Fe(%)**	**K(%)**	**Zn(%)**	**Si(%)**	**Mg(%)**
Before the experiment	99.8	0.1	0.0	0.0	0.0	0.0	0.0
After 2.5h	92.7	6.2	0.6	0.4	0.0	0.0	0.0
After 5h	88.3	9.0	2.7	0.0	0.0	0.0	0.0
After 10h	70.9	21.2	1.3	3.3	1.4	0.6	0.4

Ni electrode element concentrations					
	Ni(%)	**O(%)**	**Fe(%)**	**Si(%)**	**Al(%)**
Before the experiment	91.4	4.0	2.0	0.7	0.4
After 2.5h	76.6	18.5	0.0	0.3	0.9
After 5h	71.4	22.8	0.1	0.5	1.7
After 10h	72.6	16.9	0.3	0.5	1.6

(b)

Pd electrode nuclear balances

$$\mathrm{Pd}_{46}^{106} \rightarrow \mathrm{Ca}_{20}^{40} + \mathrm{Fe}_{26}^{56} + 10\mathrm{n}_{0}^{1}$$
$$\mathrm{Pd}_{46}^{106} \rightarrow \mathrm{Zn}_{30}^{64} + \mathrm{Si}_{14}^{28} + \mathrm{He}_{2}^{4} + 10\mathrm{n}_{0}^{1}$$
$$\mathrm{Fe}_{26}^{56} \rightarrow 3\mathrm{O}_{8}^{16} + \mathrm{He}_{2}^{4} + 4\mathrm{n}_{0}^{1}$$
$$\mathrm{Ca}_{20}^{40} \rightarrow \mathrm{O}_{8}^{16} + \mathrm{Mg}_{12}^{24}$$
$$\mathrm{Ca}_{20}^{40} \rightarrow 2\mathrm{O}_{8}^{16} + 2\mathrm{He}_{2}^{4}$$
$$\mathrm{Ca}_{20}^{40} \rightarrow \mathrm{K}_{19}^{39} + \mathrm{H}_{1}^{1}$$

Ni electrode nuclear balances

$$\mathrm{Ni}_{28}^{58} \rightarrow 3\mathrm{O}_{8}^{16} + 2\mathrm{He}_{2}^{4} + 2\mathrm{n}_{0}^{1}$$
$$\mathrm{Fe}_{26}^{56} \rightarrow 3\mathrm{O}_{8}^{16} + \mathrm{He}_{2}^{4} + 4\mathrm{n}_{0}^{1}$$
$$\mathrm{Fe}_{26}^{56} \rightarrow 2\mathrm{Al}_{13}^{27} + 2\mathrm{n}_{0}^{1}$$

(c)

Pd electrode stoichiometric balances

$$\mathrm{Pd}\ (-\ 26.6\%) = \mathrm{Ca}\ (+\ 10.0\%) + \mathrm{Fe}\ (+\ 14.1\%) + \mathrm{n}\ (+\ 2.5\%)$$
$$\mathrm{Pd}\ (-\ 2.3\%) = \mathrm{Zn}\ (+\ 1.4\%) + \mathrm{Si}\ (+\ 0.6\%) + \mathrm{He}\ (+\ 0.1\%) + \mathrm{n}\ (+\ 0.2\%)$$
$$\mathrm{Fe}\ (-\ 12.8\%) = \mathrm{O}\ (+\ 11.0\%) + \mathrm{He}\ (+\ 0.9\%) + \mathrm{n}\ (+\ 0.9\%)$$
$$\mathrm{Ca}\ (-\ 0.7\%) = \mathrm{O}\ (+\ 0.3\%) + \mathrm{Mg}\ (+\ 0.4\%)$$
$$\mathrm{Ca}\ (-\ 6.0\%) = \mathrm{O}\ (+\ 4.8\%) + \mathrm{He}\ (+\ 1.2\%)$$
$$\mathrm{Ca}\ (-\ 3.3\%) = \mathrm{K}\ (+\ 3.3\%) + \mathrm{H}\ (+\ 0.0\%)$$

Ni electrode stoichiometric balances

$$\mathrm{Ni}\ (-\ 18.8\%) = \mathrm{O}\ (+\ 15.6\%) + \mathrm{He}\ (+\ 2.6\%) + \mathrm{n}\ (+\ 0.6\%)$$
$$\mathrm{Fe}\ (-\ 0.5\%) = \mathrm{O}\ (+\ 0.4\%) + \mathrm{He}\ (+\ 0.05\%) + \mathrm{n}\ (+\ 0.05\%)$$
$$\mathrm{Fe}\ (-\ 1.2\%) = \mathrm{Al}\ (+\ 1.2\%) + \mathrm{n}\ (+\ 0.1\%)$$

The remaining two experiments (Tests 3 and 4) provided totally comparable results, thus confirming the repeatability of the four Pd-Ni experimental tests.

As noted above, the most significant chemical changes were found at the end of the experimental tests.

In Tables 3a-c and 4a-c, the Pd and Ni electrode compositional concentrations evaluated before and after the electrolytic experiments are reported for Tests 3 and 4. This data includes the nuclear and stoichiometric balances.

The phono-fission reactions postulated above can explain the chemical concentration variations and the related balances.

It is remarkable to observe that the depletion of Pd and Ni is closely counterbalanced by the increases in lighter elements and fragments with an approximation of 2.2% for the Pd electrode and of 1.3% for the Ni electrode of Test 1. Depletion of approximately 5.0% for the Pd electrode and of 3.1% for the Ni electrode of Test 2 was found. Finally, depletion of 1.1% for the Pd electrode, 0.8% for the Ni electrode, and 3.9% for the Pd electrode, 1.1% for the Ni electrode were observed for Tests 3 and 4, respectively.

5. Heat Generation and Energy Balance: A Preliminary Discussion

The aim of this section is to provide a preliminary evaluation about the thermodynamic balance related to the electrolytic experiments. In order to proceed with a correct assessment of the different physical quantities involved in the energy balance, it is essential to introduce some hypotheses about the electrolytic cell.

First of all, the input energy is linked to the electric power exchanged between the two electrodes and can be quantified by the direct electric power consumption. The corresponding electric power (E_{in}) can be calculated as the average power absorbed by the system, and it is given by direct electric measurements performed during the experiment by means of a virtual oscilloscope and a power-meter suitably programmed and developed.

The main terms of the energy transformation are: the latent heat of evaporation, the convective heat transfer, and the Stefan-Boltzmann thermal radiation.

The first term can be computed by measuring the condensed water volume and temperature. Then, the convective heat transfer can be quantified by means of thermodynamic heat exchange equations. Finally, the thermal radiation is monitored by a FLIR A300 thermographic camera focused on a pipe the excess vapor flows through, when it comes out from the reservoir.

Therefore, by evaluating the amount of electric and thermal energy emitted by the aforesaid processes, any possible energy excess could be attributed to the postulated phenomena. The measurements of the energy variation around the neutron emission peaks, shown in Figures 2 and 3, indicated an excess energy balance up to three times higher than the input energy. More detailed considerations on this topic will be discussed in a further publication.

6. Conclusions

Literature reports several examples of unexpected nuclear reactions occurring in condensed matter during electrolysis experiments characterized by particle emissions, excess heat generation, and compositional changes [9]–[36]. However, despite the large number of experimental results, a unified theory common to all of these phenomena has not yet been proposed and the common mechanism is still unknown [19], [20].

As shown in different papers devoted to so-called cold nuclear fusion, one of the principal features is the appearance of microcracks on electrode surfaces after the tests [30], [31]. Such evidence might be directly correlated to hydrogen embrittlement that could play a crucial role in the observed microcracking of the electrode host metals (Pd, Ni, Fe, etc.). The metal electrode is subjected to mechanical damage and fractures due to electrolytically produced hydrogen ions that are absorbed into the host metal; the hydrogen ions reduce the metal electrode's fracture toughness, which triggers brittle crack propagation.

Table 3. Test 3 on Pd and Ni electrodes. Element concentrations before the experiment, and after 2.5, 5, 10 hours from the beginning (a), nuclear (b) and stoichiometric (c) balances.

(a)

Pd electrode element concentrations							
	Pd(%)	**O(%)**	**Fe(%)**	**Ca(%)**	**K(%)**	**Si(%)**	**Mg(%)**
Before the experiment	99.9	0.1	0.0	0.0	0.0	0.0	0.0
After 2.5h	93.4	5.2	0.6	0.0	0.7	0.0	0.0
After 5h	86.3	8.3	1.9	0.0	0.5	0.2	0.2
After 10h	74.0	15.8	2.7	0.7	1.0	0.5	1.1

Ni electrode element concentrations					
	Ni(%)	**O(%)**	**Fe(%)**	**Si(%)**	**Al(%)**
Before the experiment	94.6	1.9	1.7	0.1	0.0
After 2.5h	87.6	11.3	0.9	0.3	0.7
After 5h	83.4	12.8	0.2	0.6	1.1
After 10h	82.0	11.9	0.0	0.5	0.9

(b)

Pd electrode nuclear balances

$$\mathrm{Pd}_{46}^{106} \rightarrow \mathrm{Ca}_{20}^{40} + \mathrm{Fe}_{26}^{56} + 10\mathrm{n}_{0}^{1}$$
$$\mathrm{Fe}_{26}^{56} \rightarrow 3\mathrm{O}_{8}^{16} + \mathrm{He}_{2}^{4} + 4\mathrm{n}_{0}^{1}$$
$$\mathrm{Ca}_{20}^{40} \rightarrow \mathrm{O}_{8}^{16} + \mathrm{Mg}_{12}^{24}$$
$$\mathrm{Ca}_{20}^{40} \rightarrow 2\mathrm{O}_{8}^{16} + 2\mathrm{He}_{2}^{4}$$
$$\mathrm{Ca}_{20}^{40} \rightarrow \mathrm{K}_{19}^{39} + \mathrm{H}_{1}^{1}$$
$$\mathrm{Ca}_{20}^{40} \rightarrow \mathrm{C}_{6}^{12} + \mathrm{Si}_{14}^{28}$$

Ni electrode nuclear balances

$$\mathrm{Ni}_{28}^{58} \rightarrow 3\mathrm{O}_{8}^{16} + 2\mathrm{He}_{2}^{4} + 2\mathrm{n}_{0}^{1}$$
$$\mathrm{Ni}_{28}^{58} \rightarrow 2\mathrm{Si}_{14}^{28} + 2\mathrm{n}_{0}^{1}$$
$$\mathrm{Fe}_{26}^{56} \rightarrow 3\mathrm{O}_{8}^{16} + \mathrm{He}_{2}^{4} + 4\mathrm{n}_{0}^{1}$$
$$\mathrm{Fe}_{26}^{56} \rightarrow 2\mathrm{Al}_{13}^{27} + 2\mathrm{n}_{0}^{1}$$

(c)

Pd electrode stoichiometric balances

$$\mathrm{Pd}\ (-25.9\%) = \mathrm{Ca}\ (+9.8\%) + \mathrm{Fe}\ (+13.7\%) + \mathrm{n}\ (+2.4\%)$$
$$\mathrm{Fe}\ (-11.0\%) = \mathrm{O}\ (+9.4\%) + \mathrm{He}\ (+0.8\%) + \mathrm{n}\ (+0.8\%)$$
$$\mathrm{Ca}\ (-1.8\%) = \mathrm{O}\ (+0.7\%) + \mathrm{Mg}\ (+1.1\%)$$
$$\mathrm{Ca}\ (-5.6\%) = \mathrm{O}\ (+4.5\%) + \mathrm{He}\ (+1.1\%)$$
$$\mathrm{Ca}\ (-1.0\%) = \mathrm{K}\ (+1.0\%) + \mathrm{H}\ (+0.0\%)$$
$$\mathrm{Ca}\ (-0.7\%) = \mathrm{C}\ (+0.2\%) + \mathrm{Si}\ (+0.5\%)$$

Ni electrode stoichiometric balances

$$\mathrm{Ni}\ (-12.2\%) = \mathrm{O}\ (+10.1\%) + \mathrm{He}\ (+1.7\%) + \mathrm{n}\ (+0.4\%)$$
$$\mathrm{Ni}\ (-0.4\%) = \mathrm{Si}\ (+0.4\%) + \mathrm{n}\ (+0.0\%)$$
$$\mathrm{Fe}\ (-0.8\%) = \mathrm{O}\ (+0.7\%) + \mathrm{He}\ (+0.05\%) + \mathrm{n}\ (+0.05\%)$$
$$\mathrm{Fe}\ (-0.9\%) = \mathrm{Al}\ (+0.9\%) + \mathrm{n}\ (+0.0\%)$$

Table 4. Test 4 on Pd and Ni electrodes. Element concentrations before the experiment, and after 2.5, 5, 10 hours from the beginning (a), nuclear (b) and stoichiometric (c) balances.

(a)

Pd electrode element concentrations							
	Pd(%)	**O(%)**	**Fe(%)**	**Ca(%)**	**K(%)**	**Si(%)**	**Mg(%)**
Before the experiment	100.0	0.0	0.0	0.0	0.0	0.0	0.0
After 2.5h	93.1	4.2	1.1	0.3	0.8	0.0	0.0
After 5h	85.7	10.2	1.2	0.7	1.0	0.3	0.6
After 10h	77.4	14.5	0.9	1.5	2.0	1.6	1.5

Ni electrode element concentrations					
	Ni(%)	**O(%)**	**Fe(%)**	**Si(%)**	**Al(%)**
Before the experiment	90.9	3.2	1.5	0.4	0.0
After 2.5h	77.1	17.3	1.0	0.7	1.3
After 5h	76.4	19.8	0.4	0.4	1.1
After 10h	74.5	13.6	0.6	2.3	1.5

(b)

Pd electrode nuclear balances

$$\mathrm{Pd}_{46}^{106} \rightarrow \mathrm{Ca}_{20}^{40} + \mathrm{Fe}_{26}^{56} + 10\mathrm{n}_{0}^{1}$$
$$\mathrm{Fe}_{26}^{56} \rightarrow 3\mathrm{O}_{8}^{16} + \mathrm{He}_{2}^{4} + 4\mathrm{n}_{0}^{1}$$
$$\mathrm{Ca}_{20}^{40} \rightarrow \mathrm{O}_{8}^{16} + \mathrm{Mg}_{12}^{24}$$
$$\mathrm{Ca}_{20}^{40} \rightarrow 2\mathrm{O}_{8}^{16} + 2\mathrm{He}_{2}^{4}$$
$$\mathrm{Ca}_{20}^{40} \rightarrow \mathrm{K}_{19}^{39} + \mathrm{H}_{1}^{1}$$
$$\mathrm{Ca}_{20}^{40} \rightarrow \mathrm{C}_{6}^{12} + \mathrm{Si}_{14}^{28}$$

Ni electrode nuclear balances

$$\mathrm{Ni}_{28}^{58} \rightarrow 3\mathrm{O}_{8}^{16} + 2\mathrm{He}_{2}^{4} + 2\mathrm{n}_{0}^{1}$$
$$\mathrm{Ni}_{28}^{58} \rightarrow 2\mathrm{Si}_{14}^{28} + 2\mathrm{n}_{0}^{1}$$
$$\mathrm{Fe}_{26}^{56} \rightarrow 2\mathrm{Al}_{13}^{27} + 2\mathrm{n}_{0}^{1}$$
$$\mathrm{Si}_{14}^{28} \rightarrow \mathrm{Al}_{13}^{27} + \mathrm{H}_{1}^{1}$$

(c)

Pd electrode stoichiometric balances

$$\mathrm{Pd}\ (-\ 22.6\%) = \mathrm{Ca}\ (+\ 8.5\%) + \mathrm{Fe}\ (+\ 11.9\%) + \mathrm{n}\ (+\ 2.1\%)$$
$$\mathrm{Fe}\ (-\ 11.0\%) = \mathrm{O}\ (+\ 9.4\%) + \mathrm{He}\ (+\ 0.8\%) + \mathrm{n}\ (+\ 0.8\%)$$
$$\mathrm{Ca}\ (-\ 2.5\%) = \mathrm{O}\ (+\ 1.0\%) + \mathrm{Mg}\ (+\ 1.5\%)$$
$$\mathrm{Ca}\ (-\ 0.2\%) = \mathrm{O}\ (+\ 0.2\%) + \mathrm{He}\ (+\ 0.0\%)$$
$$\mathrm{Ca}\ (-\ 2.0\%) = \mathrm{K}\ (+\ 2.0\%) + \mathrm{H}\ (+\ 0.0\%)$$
$$\mathrm{Ca}\ (-\ 2.3\%) = \mathrm{C}\ (+\ 0.7\%) + \mathrm{Si}\ (+\ 1.6\%)$$

Ni electrode stoichiometric balances

$$\mathrm{Ni}\ (-\ 13.9\%) = \mathrm{O}\ (+\ 11.5\%) + \mathrm{He}\ (+\ 1.9\%) + \mathrm{n}\ (+\ 0.5\%)$$
$$\mathrm{Ni}\ (-\ 2.5\%) = \mathrm{Si}\ (+\ 2.5\%) + \mathrm{n}\ (+\ 0.0\%)$$
$$\mathrm{Fe}\ (-\ 0.9\%) = \mathrm{Al}\ (+\ 0.9\%) + \mathrm{n}\ (+\ 0.0\%)$$
$$\mathrm{Si}\ (-\ 0.6\%) = \mathrm{Al}\ (+\ 0.6\%) + \mathrm{H}\ (+\ 0.0\%)$$

Based on the recent experiments carried out by the authors, a mechanical interpretation is proposed of the aforementioned phenomena induced by phono-fission reactions in the THz frequency range.

The original results reported in the present paper confirm the repeatability of the data obtained during the early experiments already published [38], [46].

In particular, neutron emission peaks up to one order of magnitude higher than the background level were measured. In addition, the EDX analyses performed on the electrode surfaces provide evidence showing that depletion of Pd and Ni appear to be almost perfectly counterbalanced by increases in lighter elements. In particular, the differences between the experimentally measured concentrations and the expected theoretical values are mainly due to the oxygen and potassium excess, which can be interpreted as an artifact of K_2CO_3 aqueous solution deposition.

It was observed that the most significant nuclear transmutations usually appeared in the latter part of the experiments and not continuously throughout their total duration, suggesting that an incubation period seems to characterize the phenomenon.

Moreover, evidence of diffused cracking emerged on the electrode surface after the experiments, emphasizing the mechanical explanation based on hydrogen embrittlement, microcracking, and terahertz phonons emitted by microcrack formation and/or propagation. These results suggest that, during the gas loading with hydrogen or deuterium, the host lattice is subjected to mechanical damage and fracture due to hydrogen ion absorption at the near surface and into the bulk electrode.

In conclusion, a preliminary evaluation in terms of heat generation has been carried out, showing an excess energy balance correlated with the major neutron emission peaks. This latter topic will be more thoroughly discussed in a subsequent publication.

Acknowledgements

This project has received funding from the European Union's Horizon 2020 research and innovation programme under grant agreement No 951974. This work reflects only the author's view, and the Commission is not responsible for any use that may be made of the information it contains.

Special thanks for their collaboration in the chemical analyses are due to Dr. Angelica Chiodoni and Dr. Salvatore Guastella. In addition, the owner of the electrolytic cell, Mr. Alessandro Goi, is gratefully acknowledged.

References

[1] F. Paneth, and K. Peters, "The Reported Conversion of Hydrogen into Helium" Nature 118: 526, (1926).
[2] M. Fleischmann, S. Pons, and M. Hawkins, "Electrochemically Induced Nuclear Fusion of Deuterium". J. Electroanal. Chem. 261: 301, (1989).
[3] T. Mizuno, "Nuclear Transmutation: The Reality of Cold Fusion". Infinite Energy Press. (1998).
[4] T. Ohmori, and T. Mizuno, "Strong Excess Energy Evolution, New Element Production, and Electromagnetic Wave and/or Neutron Emission in Light Water Electrolysis with a Tungsten Cathode". Infinite Energy. Issue 20: 14–17, (1998).
[5] T. Mizuno, T. Akimoto, and T. Ohmori, "Confirmation of anomalous hydrogen generation by plasma electrolysis". 4th Meeting of Japan CF Research Society. 2003. Iwate, Japan: Iwate University.
[6] P.A. Mosier-Boss, et al., "Use of CR-39 in Pd/D co-deposition experiments". Eur. Phys. J. Appl. Phys. 40: 293–303, (2007).
[7] P.A. Mosier-Boss, et al., "Comparison of Pd/D co-deposition and DT neutron generated triple tracks observed in CR-39 detectors". Eur. Phys. J. Appl. Phys. 51(2): 20901–20911, (2010).
[8] S. Szpak, P.A. Mosier-Boss, C. Young, F.E. Gordon, "The effect of an external electric field on surface morphology of co-deposited Pd/D films". J. Electroanal. Chem. 580(2): 284–290, (2005).
[9] P.W. Bridgman, "The breakdown of atoms at high pressures". Phys. Rev. 29: 188–191, (1927)
[10] R.E. Batzel, G.T. Seaborg, "Fission of medium weight elements". Phys Rev 82: 607–615, (1951).

[11] D.C. Borghi, D.C. Giori, A. Dall'Olio, "Experimental Evidence on the Emission of Neutrons from Cold Hydrogen Plasma", Proceedings of the International Workshop on Few-body Problems in Low-energy Physics, Alma-Ata, Kazakhstan, 147-154, (1992); Unpublished Communication (1957); Comunicacao n. 25 do CENUFPE, Recife Brazil, (1971).
[12] K. Diebner, "Fusionsprozesse mit Hilfe konvergenter Stosswellen – einige aeltere und neuere Versuche und Ueberlegungen", Kerntechnik, 3: 89–93, (1962).
[13] C.B. Fulmer, et al. "Evidence for photofission of iron". Phys Rev Lett 19: 522–523, (1967).
[14] T. Y. Goradovskii, "Hard radiation from solids failing in shear." JETP Lett 5: 64-67, (1967).
[15] S. Kaliski, "Bi-conical system of concentric explosive compression of D-T", J. Tech. Phys. 19: 283–289, (1978).
[16] F. Winterberg, "Autocatalytic fusion–fission implosions", Atomenergie-Kerntechnik. 44: 146, (1984).
[17] B. V. Derjaguin, et al., "Titanium fracture yields neutrons? " Nature 34: 492, (1989).
[18] J.O'M. Bockris, G.H. Lin, R.C. Kainthla, N.J.C. Packham, and O. Velev, "Does Tritium Form at Electrodes by Nuclear Reactions?", The First Annual Conference on Cold Fusion. National Cold Fusion Institute, University of Utah Research Park, Salt Lake City, (1990).
[19] G.Preparata, "Some theories of cold fusion: A review", Fusion Tech. 20: 82, (1991).
[20] G. Preparata, "A new look at solid-state fractures, particle emissions and ≪cold≫ nuclear fusion", Il Nuovo Cimento. 104 A: 1259–1263, (1991).
[21] R.L. Mills, and P. Kneizys, "Excess heat production by the electrolysis of an aqueous potassium carbonate electrolyte and the implications for cold fusion", Fusion Technol. 20: 65, (1991).
[22] R. Notoya, and M. Enyo, "Excess Heat Production during Electrolysis of H_2O on Ni, Au, Ag and Sn Electrodes in Alkaline Media", Proc. Third International Conference on Cold Fusion, Nagoya Japan: Universal Academy Press, Inc., Tokyo, Japan, (1992).
[23] M.H. Miles, R.A. Hollins, B.F. Bush, J.J. Lagowski, and R.E. Miles, "Correlation of Excess Power and Helium Production during D_2O and H_2O Electrolysis using Palladium Cathodes", J. Electroanal. Chem. 346: 99–117, (1993).
[24] R.T. Bush, and R.D. Eagleton, "Calorimetric studies for several light water electrolytic cells with nickel fibrex cathodes and electrolytes with alkali salts of potassium, rubidium, and cesium", Fourth International Conference on Cold Fusion. Lahaina, Maui. Electric Power Research Institute 3412 Hillview Ave., Palo Alto, CA 94304. 13, (1993).
[25] M. Fleischmann, S. Pons, G. Preparata, "Possible Theories of cold Fusion", Nuovo Cimento. Soc. Ital. Fis. A. 107: 143, (1994).
[26] R. Sundaresan, and J.O.M. Bockris, "Anomalous reactions during arcing between carbon rods in water", Fusion Technol. 26: 261, (1994).
[27] Y. Arata, Y. Zhang, "Achievement of solid-state plasma fusion ("cold-fusion")", Proc. Jpn Acad. 71: 304–309, (1995).
[28] S.R. Little, H.E. Puthoff, and M.E. Little, "Search for Excess Heat from a Pt Electrode Discharge in K_2CO_3-H_2O and K_2CO_3-D_2O Electrolytes", Infinite Energy 5: 34, (1998).
[29] H.E. Ransford, "Non-Stellar nucleosynthesis: Transition metal production by DC plasma-discharge electrolysis using carbon electrodes in a non-metallic cell", Infinite Energy. 4(23): 16, (1999).
[30] E. Storms, "Excess power production from platinum cathodes using the Pons-Fleischmann effect. 8th International Conference on Cold Fusion", Lerici (La Spezia). Italian Physical Society, Bologna, Italy. p. 55–61, (2000).
[31] E. Storms, "Science of Low Energy Nuclear Reaction: A Comprehensive Compilation of Evidence and Explanations About Cold Fusion", World Scientific Publishing Co. Pte. Ltd. Singapore, (2007).
[32] J. Warner, J. Dash, and S. Frantz, "Electrolysis of D2O with titanium cathodes: enhancement of excess heat and further evidence of possible transmutation", The Ninth International Conference on Cold Fusion. Tsinghua University, Beijing, China. p. 404, (2002).
[33] M.F. Fujii, et al., "Neutron emission from fracture of piezoelectric materials in deuterium atmosphere", Jpn. J. Appl. Phys., 41: 2115–2119, (2002).
[34] A.G. Lipson, et al. "DD reaction enhancement and X-ray generation in a high-current pulsed glow discharge in deuterium with titanium cathode at 0.8–2.45 kV." Journal of Experimental and Theoretical Physics 100.6, (2005).
[35] M. Swartz, "Three Physical Regions of Anomalous Activity in Deuterated Palladium", Infinite Energy. 14: 19–31, (2008).
[36] M. Kanarev, and T. Mizuno, "Cold fusion by plasma electrolysis of water", New Energy Technologies, Issue 1: 5–10, (2002).

[37] R.P. Gangloff, "Hydrogen-assisted cracking", in Comprehensive Structural Integrity, I. Milne, R.O. Ritchie, B. Karihaloo (Editors), Pergamon, 31–101, (2003).
[38] A. Carpinteri, G. Lacidogna, A. Manuello (Editors), "Acoustic, Electromagnetic, Neutron Emissions from Fracture and Earthquakes", Springer, 2015.
[39] F. Cardone, R. Mignani, "Energy and Geometry", World Scientific. Singapore, chap. 10, (2004).
[40] F. Cardone, R. Mignani, "Deformed spacetime", Chapters 16 and 17. Springer, Dordrecht, (2007)
[41] A. Carpinteri, F. Cardone, G. Lacidogna, "Piezonuclear neutrons from brittle fracture: Early results of mechanical compression tests", Strain. 45: 332–339, (2009).
[42] F. Cardone, A. Carpinteri, G. Lacidogna, "Piezonuclear neutrons from fracturing of inert solids", Physics Letters A. 373: 4158−4163, (2009).
[43] A. Carpinteri, F. Cardone, G. Lacidogna, "Energy emissions from failure phenomena: Mechanical, electromagnetic, nuclear", Experimental Mechanics. 50: 1235−1243, (2010).
[44] A. Carpinteri, G. Lacidogna, A. Manuello, O. Borla, "Piezonuclear fission reactions: evidences from microchemical analysis, neutron emission, and geological transformation", Rock Mechanics and Rock Engineering. 45: 445–459, (2012).
[45] A. Carpinteri, G. Lacidogna, A. Manuello, O. Borla, "Piezonuclear fission reactions from earthquakes and brittle rocks failure: Evidence of neutron emission and nonradioactive product elements", Experimental Mechanics. 53: 345–365, (2013).
[46] A. Carpinteri, O. Borla, A. Manuello, D. Veneziano and A. Goi, "Hydrogen Embrittlement and Piezonuclear Reactions in Electrolysis Experiments", J. Condensed Matter Nucl. Sci. 15: 162–182, (2015).
[47] A. Carpinteri, O. Borla, G. Lacidogna, A. Manuello, "Neutron emissions in brittle rocks during compression tests: Monotonic vs. cyclic loading", Physical Mesomech., 13: 264-274, (2010).
[48] A. Carpinteri, G. Lacidogna, A. Manuello, O. Borla, "Energy emissions from brittle fracture: Neutron measurements and geological evidences of piezonuclear reactions", Strength, Fracture and Complexity, 7: 13–31, (2011).
[49] A. Carpinteri, A. Chiodoni, A. Manuello, R. Sandrone, "Compositional and microchemical evidence of piezonuclear fission reactions in rock specimens subjected to compression tests", Strain, Vol. 47(2): 267–281, (2011).
[50] A. Carpinteri, A. Manuello, "Geomechanical and geochemical evidence of piezonuclear fission reactions in the Earth's Crust", Strain, Vol. 47(2): 282–292, (2011).
[51] A. Carpinteri, G. Lacidogna, O. Borla, A. Manuello, G. Niccolini, "Electromagnetic and neutron emissions from brittle rocks failure: Experimental evidence and geological implications", Sadhana, 37: 59–78, (2012).
[52] A. Carpinteri, O. Borla, "Nano-scale fracture phenomena and TeraHertz pressure waves as the fundamental reasons for geochemical evolution", Strength, Fracture and Complexity, 11: 149–168, (2018).
[53] A. Carpinteri, O. Borla, "Fracto-emissions as seismic precursors", Engineering Fracture Mechanics, 177: 239–250, (2017).
[54] A. Carpinteri, O. Borla, "Acoustic, electromagnetic, and neutron emissions as seismic precursors: The lunar periodicity of low-magnitude seismic swarms", Engineering Fracture Mechanics, 210: 29–41, (2019).
[55] U. Lucia, and A. Carpinteri, "GeV plasmons and spalling neutrons from crushing of iron-rich natural rocks", Chemical Physics Letters, 640: 112–114, (2015).
[56] P.L. Hagelstein, D. Letts, D. Cravens, "Terahertz difference frequency response of PdD in two-laser experiments". J Cond Mat Nucl Sci 3: 59, (2010).
[57] P.L. Hagelstein, I.U. Chaudhary, "Anomalies in fracture experiments and energy exchange between vibrations and nuclei", Meccanica, 50: 1189–1203, (2015).
[58] A. Widom, J. Swain, Y.N. Srivastava, "Neutron production from the fracture of piezoelectric rocks". J Phys G: Nucl Part Phys 40(15006):1–8, (2013).
[59] A. Widom, J. Swain, Y.N. Srivastava, "Photo-disintegration of the iron nucleus in fractured magnetite rocks with magnetostriction", Meccanica, 50: 1205–1216, (2015).
[60] A. Widom, Y.Srivastava, J. Swain, G. de Montmollin, L. Rosselli, "Reaction products from electrode fracture and Coulomb explosions in batteries", Engineering Fracture Mechanics 184: 88–100, (2017).
[61] A. Widom, Y. Srivastava, J. Swain, G.de Montmollin, "Tensile and explosive properties of current carrying wires", Engineering Fracture Mechanics 197: 114–127, (2018).